

Biophysical Studies on the Interaction of Insulin with a Cationic Gemini Surfactant

M. Pirhaghghi¹, A.A. Saboury¹, F. Najafi², P.S. Pourhosseini^{*3}, and H. Ghourchian¹

¹*Institute of Biochemistry and Biophysics, University of Tehran, Tehran, Islamic Republic of Iran*

²*Department of Resin and Additives, Institute for Color Science and Technology, Tehran, Islamic Republic of Iran*

³*Faculty of Biological Sciences, Alzahra University, Tehran, Islamic Republic of Iran*

Received: 22 January 2015 / Revised: 16 February 2015 / Accepted: 9 March 2015

Abstract

A novel quaternary ammonium-based cationic gemini surfactant (S_6) having 1,6-dibromo hexane as a spacer, have been used and its interaction with insulin in aqueous solution (pH, 7.40) was investigated by several methods including fluorescence spectroscopy, UV-Vis spectroscopy, circular dichroism, dynamic light scattering, ζ -potential measurements, conductivity and transmission electron microscopy. Conductometry and fluorescence studies confirmed the complex formation between S_6 and insulin. TEM micrographs revealed that the S_6 micelles were of spherical shape with size distribution between 101-140 nm. The critical micelle concentration and some physicochemical properties were determined by conductance measurements. Fluorescence quenching studies in the presence of acrylamide indicated that in the protein-surfactant interaction the solvent accessibility of Tyr residues is reduced. Furthermore CD experiments (far- and near-UV CD) showed that, the content of alpha-helix increases with increasing S_6 concentration and some conformational changes occur in protein structure. The results from dynamic light scattering and ζ -potential measurements showed that insulin charge neutralization and hexamer dissociation take place in the presence of surfactant. Altogether, the S_6 cationic Gemini surfactant can be considered as a candidate for insulin delivery.

Keywords: Cationic gemini surfactant; spectroscopic studies; DLS; zeta potential; conductometry.

Introduction

Proteins play an important role in living organisms. They can bind to various types of ligands such as surfactants, metal ions, drugs and so on [1-4]. In the recent years, surfactants have been developed and protein-surfactant interaction studies have gained great attentions. Surfactants can interact with proteins and

make them stable or denature. Most of studies on surfactant-protein interactions is focused on single-chain surfactants [5-10].

Gemini or dimeric surfactants are amphiphilic molecules, whose molecule consists of two head groups, two hydrophobic chains and one spacer group. Each of the head groups, jointed to a hydrophobic tail (similar to

* Corresponding author: Tel: +982185692718; Fax: +982188058912; Email: p.pourhosseini@alzahra.ac.ir

conventional surfactants) and these two parts are connected together by a spacer group [11, 12]. In the recent years, gemini surfactants have been well developed compared with conventional surfactants because of their superior characteristics, such as low Krafft temperature, low critical micelle concentration (cmc), much lower C_{20} values, unusual viscosity behavior, specific aggregation structures, stronger interaction with oppositely charged surfactants at the aqueous solution/air interface and so on. [13]. They have been widely used in the fields of protein study [14, 15], gene therapy [16-18], soil remediation, enhanced oil recovery [19], making biosensors [20], and drug entrapment [21]. However, interactions of proteins with double-chain surfactants have been less studied [22-24].

Insulin is a small peptide hormone (51 residues) and deficiency in its secretion causes the diabetes mellitus. Human insulin consists of two chains (A-chain and B-chain) that are connected by two disulfide bonds. An additional inter-chain disulfide bond exists in the A-chain. Under specific acidic and pH conditions, insulin may exist as a mixture of hexamer, tetramer, dimer and monomer in solution [25-28]. Two zinc ions bind to three His B¹⁰ residues, which results in hexamer formation. The hexamer is the most stable form of insulin [25, 26]. From the view point of the aromatic amino acids, insulin has 4 tyrosines and 3 phenylalanines and no tryptophan residues.

In the present work, a novel cationic gemini surfactant having 1, 6 di-bromo hexane as a spacer is used to prepare nanoparticles as drug delivery vehicles. There is a lack of study on the interaction of dimeric (gemini) surfactants with insulin. Therefore conductometry, fluorescence spectroscopy, UV-Vis spectroscopy, circular dichroism, dynamic light scattering, ζ -potential and transmission electron microscopy were used to study the interaction of this gemini surfactant with Insulin (as a peptide drug).

Materials and Methods

Protein and buffer

Human medicinal insulin (regular) was purified by dialysis against buffer, as described previously [29]. The concentration of insulin was kept constant (0.2 mg/mL) throughout the study. A new cationic gemini surfactant (S_6 , MW of 4867 Da) was used. All gemini surfactant and insulin solutions were prepared in Phosphate Buffered Saline (PBS), pH 7.40. The buffer was prepared by mixing 8.0g/l of NaCl, 0.2g/l of KCl, 1.44g/l of Na_2HPO_4 and 0.24g/l of KH_2PO_4 in deionized water [30]. The cationic gemini surfactant (S_6), was

dispersed in PBS, pH 7.40, then sonicated 22 min in 20°C ultrasonic water bath, to obtain a homogenized dispersion.

All other reagents (Merck, Darmstadt, Germany) were used without further purification.

Preparation of surfactant/protein samples

In order to acrylamide quenching, dynamic light scattering (DLS), ζ -potential measurements, circular dichroism and thermal stability measurements, we provided different molar ratios of surfactant to protein as $[S_6]/[Ins]$: 0, 3, 5, 7, 9, 10 in which the protein concentration was constant (0.2 mg/ml). Samples were incubated 30 min, before taking the measurements to obtain stable solutions. The samples without protein were used as reference solutions for circular dichroism and thermal stability measurements.

Conductivity measurements

The conductance of S_6 surfactant solutions in PBS, pH 7.40 in the absence and presence of insulin were measured by a LCR meter (HM8118, HAMEG instrument, Germany). The instrument was set at 72Hz and $25.0 \pm 0.1^\circ C$. The conductivity cell was calibrated with 0.01M KCl standard solutions and the cell constant was measured 1.06-cm^{-1} . To determine the critical micelle concentration (CMC), the buffer was successively titrated by the surfactant solution (30 mg/ml) and the conductance was measured after each titration. In order to determine the surface properties of S_6 micelles in the presence of insulin, the experiment was repeated in the same way by titration of a 0.2mg/ml protein solution with surfactant.

Morphology studies

A drop of the S_6 solution was placed on a Formvar-coated copper grid (75×300-mesh) and stained with 2% (w/v) uranyl acetate [36]. Micelles were observed using a transmission electron microscope (TEM) (EM10C, Zeiss, Germany) with the accelerating voltage of 80kV.

Fluorescence measurements

Fluorescence measurements were recorded in a Varian Cary 100 Bio spectrophotometer at $25 \pm 0.1^\circ C$, in 1.0-cm path length quartz cell. Intrinsic tyrosine fluorescence of insulin solution was excited at 276 nm and emission were recorded between 285 and 350 nm. Both the excitation and emission slits were set at 5 nm and the scan rate was 600nm/min. The reference sample consisting of the buffer and the surfactant, did not give any fluorescence signal. Insulin solution (0.2mg/ml) was manually titrated with a micropipette from a stock solution of S_6 gemini surfactant (3mg/ml).

Table 1. Determination of physicochemical properties of S₆ micelles in the absence and presence of insulin.

Sample	In the absence of insulin				In the presence of insulin				
	α (%)	β (%)	CMC (μ M)	CAC (μ M)	PSP (μ M)	M (mg)	G_{mic}^{ins} (kJ/mol)	G_{agg}^{ins} (kJ/mol)	ΔG_{PS}^{ins} (kJ/mol)
S ₆	16.4	83.6	13.15	6.5	30.4	3.5	-38.72	-40.19	-2.12

Acrylamide quenching studies were conducted by adding aliquots from an acrylamide stock solution (4.0 M) to each sample ([S₆]/[Ins]: 0, 3, 5, 7, 9, 10) and the emission was measured immediately at 303 nm. Titrations were performed so as the concentrations of acrylamide varied from 0-500 mM.

UV-Vis absorption measurements

Thermal denaturation curves of insulin upon interaction with different concentrations of S₆ were obtained by Varian Carry Eclipse UV-Vis spectrophotometer, at 25.0 ± 0.1°C. The quartz cell path length was 1.0-cm. Samples were prepared so as to give a [S₆]/[Ins] molar ratios: 0, 3, 5, 7, 9, 10. The absorbance at 276 nm were recorded in the temperature range of 25 to 95°C. The rate of temperature rise was 2 °C/min. Pace analysis was used to calculate the standard free energy change of 25°C ($\Delta G^\circ(298K)$) as thermal stability parameter [31].

Circular dichroism (CD) measurements

Circular dichroism spectra were recorded in an Aviv 215 circular dichroism spectrophotometer at 25.0±0.1°C, using a bandwidth of 1.0 nm. In far-UV CD condition (190-250 nm), a quartz cell of 0.1-cm path length was used and in the near-UV CD region (250-320 nm), measurements were made in a quartz cell of 1.0-cm path length. The reference samples spectra were subtracted from the samples spectra and CD results are expressed as molar ellipticity, θ (deg cm² dmol⁻¹). The secondary structure contents of the samples were estimated using the CDNN program related to the instrument. Data were further analyzed using phase diagrams as described elsewhere [32, 33].

Dynamic light scattering and ζ -potential measurements

The size and zeta potential measurements were carried out by Zetaplus Instrument (90Plus/BIMAS, Zetaplus, USA). The samples ([S₆]/[Ins]: 0, 3, 5, 7, 9, 10) were filtered prior to measurements directly into the cell. The filter used was a 0.22 μ m syringe filter (GVS, USA). The cell path length was 1.0-cm for both measurements. All the measurements were carried out at 25.0±0.1°C.

The wavelength of the laser beam was 657.0 nm and the scattering angle was 90°. Data were analyzed with the software supplied by the instrument. Each sample

was measured by 5 individual runs. The time of each run was 30s for DLS and 15 cycles for ζ -potential measurements. The outlier data were removed and the mean results were accepted as the final ζ -potential and hydrodynamic diameters (D_h). The corresponding diameters (D_h) and the zeta potentials were calculated using the Stoke-Einstein relationship [34] and the Smoluchowski model [35], respectively, by the instrument.

Results and Discussion

Determination of physicochemical properties by conductometry

The critical micelle concentration (CMC) and degree of micellar ionization (α) was measured using conductometry. Fig. 1A shows the plot of specific conductivity (κ) versus S₆ concentration for S₆/PBS system. It can be seen that with increasing surfactant concentration, κ increases steeply; then a break point in the curve occurs and the slope of the curve decreases thereafter. The intersection point of these two linear parts indicates the CMC of S₆, according to the Williams method [37]. The ratio of the slopes of linear parts above and below the break point (A_1/A_2) was used to calculate the degree of micelle ionization (α). The degree of counter-ion binding to micelles (β) can be obtained by Eq. 1 [1]:

$$\beta = 1 - \alpha \quad \text{Eq. 1}$$

Results are listed in Table 1.

Fig. 1B shows the effect of insulin on specific conductivity of surfactant solution. The plot displays two break points reflecting the surfactant-protein interactions. The first break point indicates the critical aggregation concentration (CAC) where the surfactant monomer-insulin interaction takes place. The second break point shows the polymer saturation point (PSP) where the micelle-insulin interaction occurs. PSP implies the protein surface has been saturated by the S₆ monomer. Actually, the PSP can be equivalent with CMC in the presence of insulin. Under these conditions, the possibility of micelle formation decreases. From Fig. 1B the ratio of B₂/B₁ gives the ionization degree of insulin-surfactant complexes (α_1), while B₃/B₁ is related to ionization of free micelles (α_2) [1].

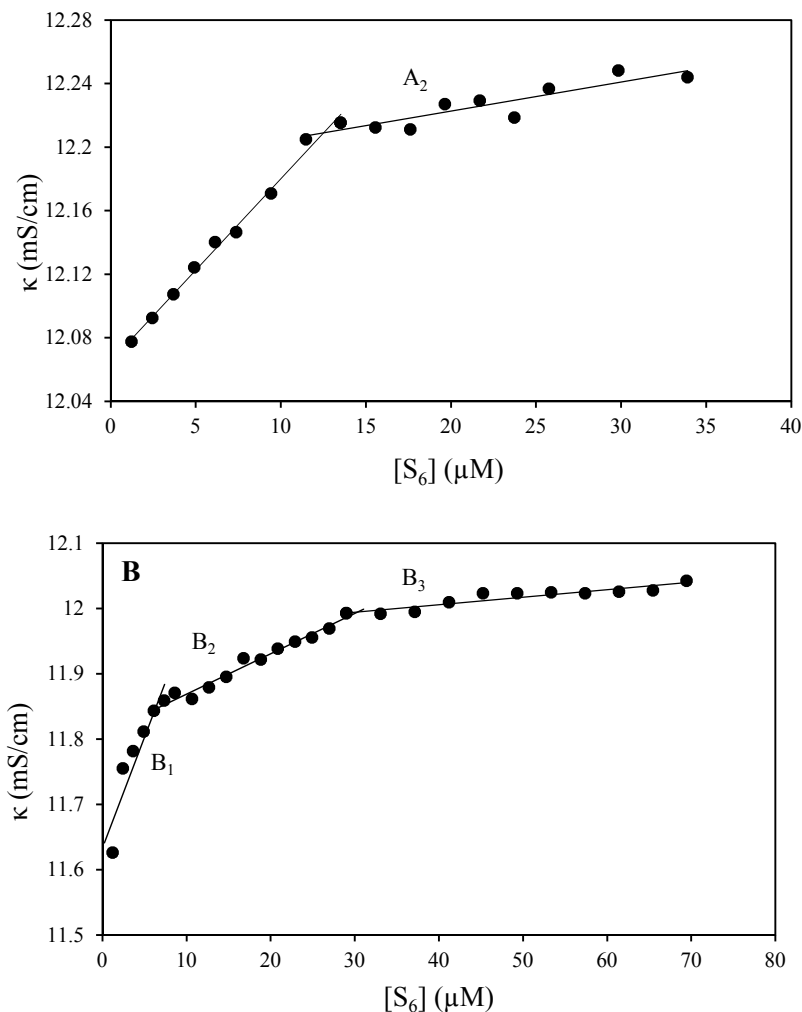


Figure 1. Plot of specific conductivity (κ) versus S_6 concentration in the absence (A) and presence (B) of insulin at 298K. S_6 concentration varies from zero to 34.0 μM and zero to 69.48 μM for A and B plots, respectively.

The standard free energy of micellization (ΔG_{mic}°), the standard free energy of aggregation (G_{agg}°), “the standard Gibbs energy for the transference of 1 mol of surfactant molecules from unperturbed micelles (that is, in the absence of protein) to protein-bound micelles (G_{PS}°)” and “the amount of surfactant, in grams, bound per gram of protein at PSP (in saturation conditions)” (M parameter) was calculated according to the following equations [1]:

$$G_{mic}^\circ = RT (1/2+\beta)\ln CMC - RT/2 \ln 2, \beta=1-\alpha \quad \text{Eq.2}$$

$$G_{agg}^\circ = RT (1/2+\beta)\ln CAC - RT/2 \ln 2, \beta=1-\alpha_1 \quad \text{Eq.3}$$

$$G_{PS}^\circ = \Delta G_{agg}^\circ - \Delta G_{mic}^\circ \quad \text{Eq.4}$$

$$M = (PSP - CAC) / [\text{Protein}] \quad \text{Eq.5}$$

Where R is the gas constant and T is the absolute temperature. All the parameters of micelle structure and its interaction with insulin are listed in Table 1.

TEM images of S_6 micelles

Understanding the shape and size distribution of the micellar carries have great importance in drug delivery processes. Fig. 2 shows the negatively stained-TEM images of S_6 micelles. As can be seen, the micelles are spherical with the size distribution between 101-140 nm. The image was taken with a magnification of 20000x.

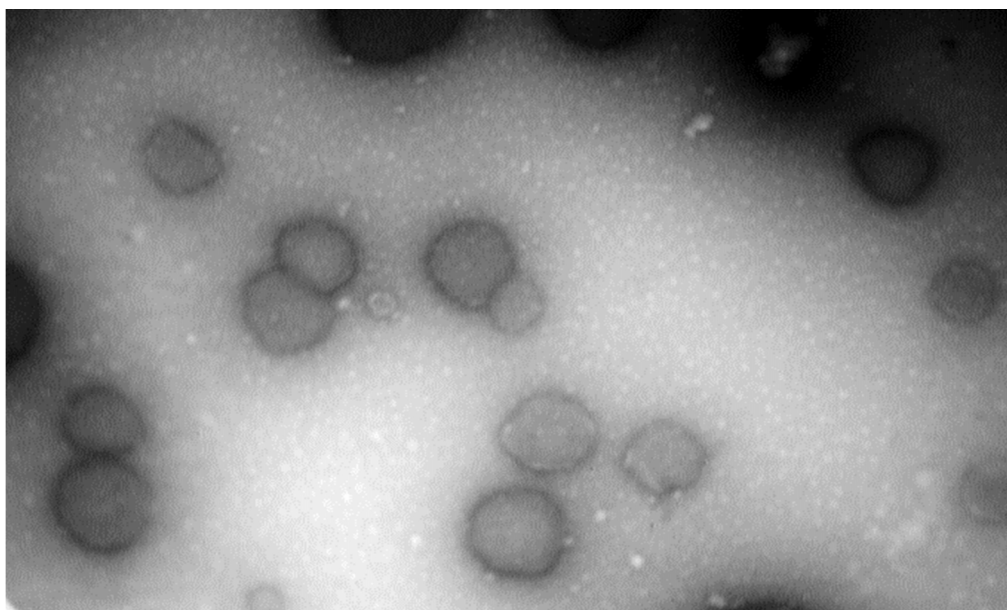


Figure 2. TEM image of S_6 micelles (7.0 mg/ml) in PBS (pH,7.40) (negative-staining, magnification: 20000x).

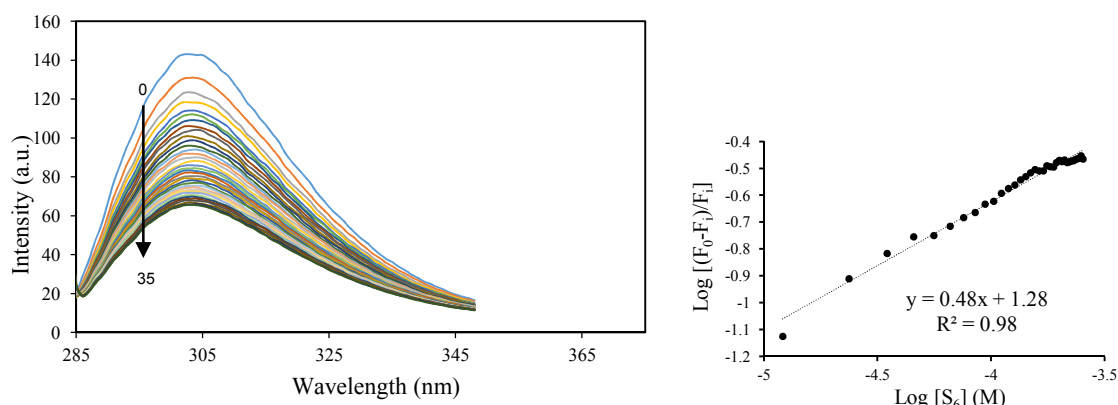


Figure 3. Fluorescence spectra of insulin (0.2 mg/ml) at different S_6 concentrations. The S_6 concentration (for curves 0 \rightarrow 35) varies from zero to 253.8 μ M. The inset is the diagram of $\text{Log} [(F_0-F_i)/F_i]$ versus $\text{Log} [S_6]$ in order to obtain the association constant (K_a). The intercept represents the logarithm of the association constant.

Intrinsic fluorescence emission

Fluorescence spectroscopy was used to monitor the structural changes of insulin induced by interactions with S_6 . The intrinsic fluorescence spectra of insulin in the absence and presence of different concentrations of S_6 are shown in Fig. 3. It displays that S_6 acts as a fluorescence quencher for insulin and the fluorescence intensity decreases upon addition of S_6 , indicating the formation of complex between the protein and the surfactant. It is also observed that there is no shift in the maximum emission wavelength, hence the polarity of tyrosine environment cannot be explained. The diagram of $\text{Log} [(F_0-F_i)/F_i]$ versus $\text{Log} [S_6]$ was plotted (Fig. 3 inset), according to Eq. 6. This diagram is linear and the

intercept was used to calculate the association constant (K_a).

$$\text{Log} [(F_0-F_i)/F_i] = \text{Log} K_a + n \text{Log} [S_6] \quad \text{Eq. 6}$$

Where F_0 and F represent the fluorescence intensity in the absence and the presence of quencher, n is number of binding sites and $[S_6]$ is the concentration of S_6 . The value of K_a obtained 19 M^{-1} . Then, the free energy of the surfactant and insulin interactions ($G^\circ(298)$), obtained from Eq. 7 [38]:

$$G^\circ = -RT \ln K_a \quad \text{Eq. 7}$$

The value of $G^\circ(298)$ obtained, -7.3 kJ/mol, indicating that the spontaneous interactions take place.

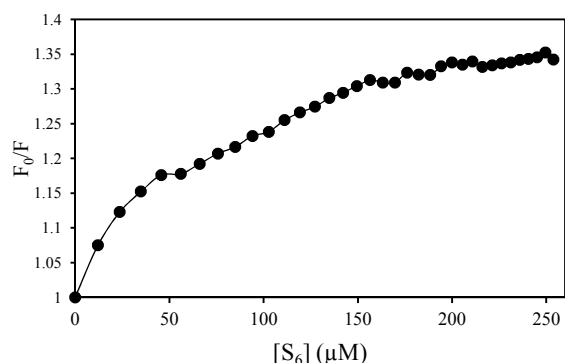


Figure 4. The Stern-Volmer plot of insulin as a function of surfactant concentration, from intrinsic fluorescence spectra.

The insulin fluorescence is dominated by four tyrosine (Tyr) residues. The Stern-Volmer equation (Eq. 8) is used to determine the fluorescence quenching mechanism [39]:

$$\frac{F_0}{F} = (1 + K_{SV}[Q])(1 + K_{eq}[Q]) \quad \text{Eq. 8}$$

Where K_{SV} represent the Stern-Volmer quenching constant, K_{eq} is the equilibrium constant and $[Q]$ is the concentration of the quencher (S_6). The first sentence indicates, dynamics quenching and the second term relates to the static quenching.

Fig. 4 shows the Stern-Volmer plot, which has a downward curvature suggesting both the dynamic and static quenching. It indicates the complex formation between S_6 and insulin which is also confirmed by other experiments of this study (conductivity measurements as well as UV-Vis spectroscopy (data are not shown)).

The secondary and tertiary structural changes in the presence of surfactant

Circular dichroism can be used to study the secondary structural changes of proteins in the presence of ligands. Insulin exhibits a negative peak in the far-UV CD spectrum at 209 nm and a shoulder at around 222 nm, which is characteristic of α -helix structure [40]. Alteration of ellipticity around these wavelengths, indicates the changes in the helical content of the protein. Fig. 5A shows far-UV CD spectra of native insulin in the absence and presence of the surfactant. Further, the contents of the secondary structure of insulin with and without surfactant, normalized to 100%, are given in Table 2. It is observed that in the presence of surfactant, the content of α -helix increases while that of β -structure and random coil decreases, which indicates that the surfactant changes the secondary structure of insulin. [22].

Near-UV CD was performed to determine the tertiary and quaternary structural changes of insulin in the presence of the surfactant. As is shown in Fig. 5B, the

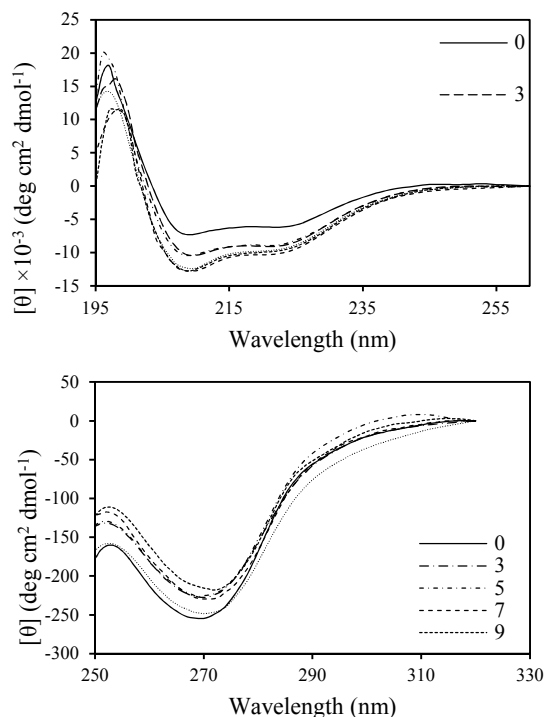


Figure 5. Far-UV CD (A) and near-UV CD (B) spectra of insulin in the interaction with different surfactant concentrations ($[S_6]/[Ins]=0, 3, 5, 7, 9, 10$) at 298K.

Table 2. The secondary structure content of insulin in the interaction with different surfactant concentration at 298K.

Samples	Helix (%)	Beta- Structure (%)	Random-Coil (%)
[S ₆]/[Ins]= 0	25.4	37.8	36.8
[S ₆]/[Ins]= 3	29.6	35.5	34.9
[S ₆]/[Ins]= 5	32.0	34.3	33.7
[S ₆]/[Ins]= 7	30.4	36.8	32.8
[S ₆]/[Ins]= 9	29.1	37.8	33.1
[S ₆]/[Ins]= 10	33.6	34.8	31.6

native hexameric protein exhibits a negative peak with a minimum at 270 nm and a small peak at 253 nm which are characteristics of tyrosine and phenylalanine residues, respectively [40, 41]. In the presence of various concentrations of the gemini surfactant, the intensity of near-UV CD signal decreases but there is no significant change in the overall shape of the spectra. The range of the ellipticity changes, is -248.50 to -214.50 deg cm² dmol⁻¹ at 270 nm. According to the results, with increasing the surfactant concentration partial changes occur in the tertiary structure of the insulin. The decrease in near-UV CD signal on the interaction with the surfactant, could be a sign of hexamer dissociation, [41, 43 and 44].

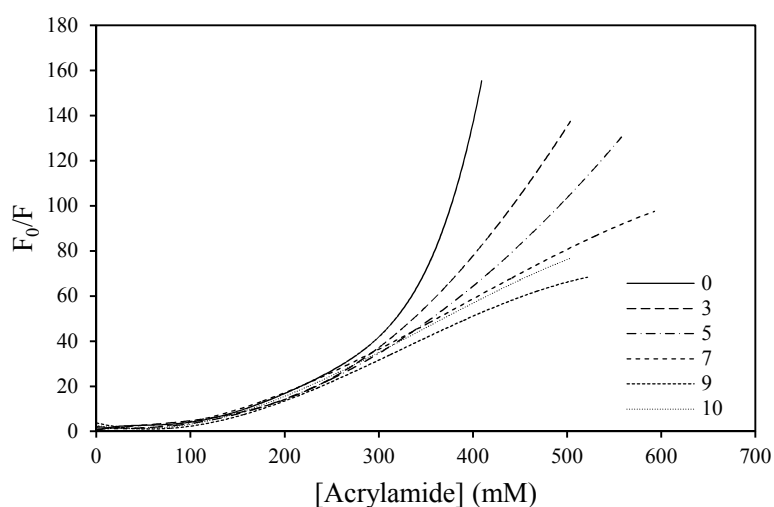
Phase diagrams can be useful tools, to get more detailed analysis of fluorescence and CD data. For CD spectroscopy, the phase diagrams (*supporting information*) (Supporting information is available at p.pourhosseini@alzahra.ac.ir), Fig. S1 A, S1 B and S2) show that, in the presence of the surfactant, there are five distinct structures with different conformations and three distinct species with different secondary

structures. Moreover, the changes in the tertiary and secondary structures of insulin start together, however these changes are not equal at higher surfactant concentrations.

Effect of S₆ on acrylamide quenching

Further information about the Tyr location and the structural changes of insulin in S₆-insulin complex was obtained from fluorescence quenching experiments. Fig. 6 shows the Stern-Volmer plots for acrylamide quenching of insulin in the absence and presence of the surfactant. It is observed that upon increasing surfactant concentration (from [S₆]/[Ins]= 0 to 10) the slope of the curves gradually decrease, suggesting that the solvent accessibility of Tyr are reduced. On the other hand, the far-UV CD data showed that the surfactant increases the helical content of insulin. Since most of the tyrosine residues of insulin are located in the α -helix structures, the reduced accessibility of tyrosines in quenching experiment is in agreement with the far-UV CD data.

Thermal Stability of insulin upon interaction with S₆

**Figure 6.** Stern-Volmer plots of insulin as a function of S₆ surfactant concentration at 298K, from acrylamide quenching studies.

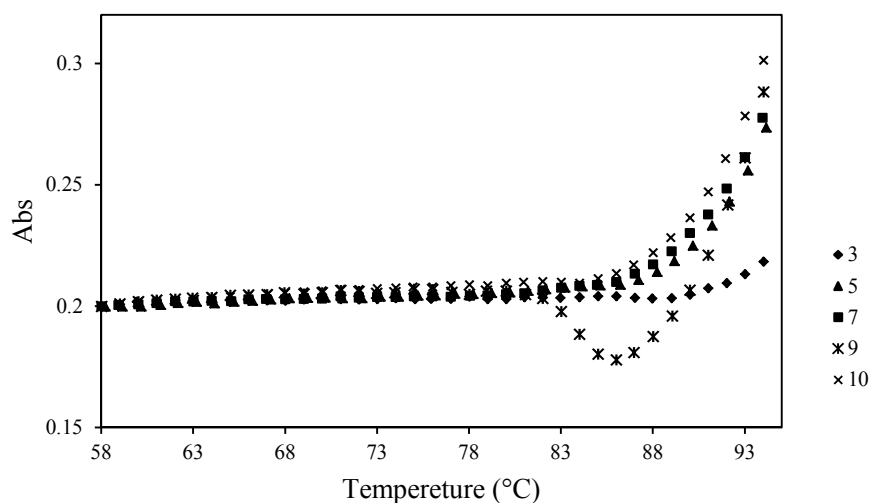


Figure 7. Thermal denaturation curves of insulin in different S_6 concentrations ($[S_6]/[Ins]= 0, 3, 5, 7, 9, 10$). The absorbance was recorded at 276 nm against temperature.

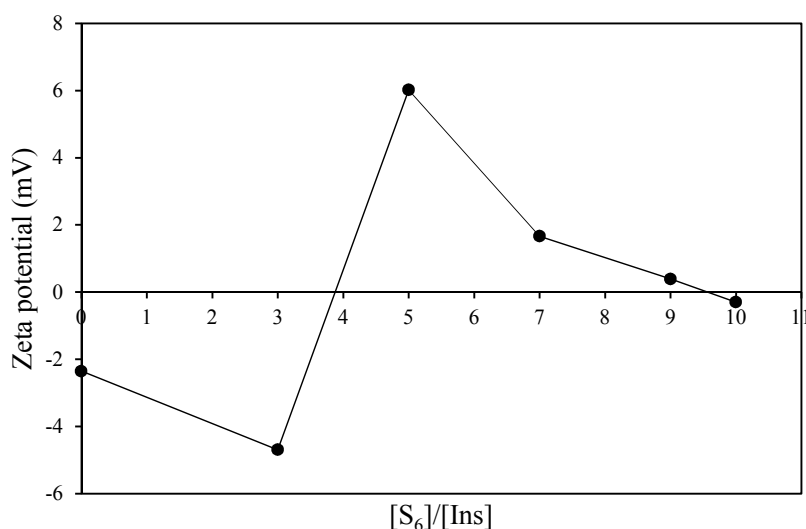


Figure 8. Zeta potential plot at different molar ratio ($[S_6]/[Ins]$) for insulin-micelle complex.

Thermal stability of insulin in the presence of S_6 was studied by UV-vis spectroscopy. The melting temperature of the protein was obtained 70 (*supporting information¹, Fig. S3*), which is confirmed by other studies [29]. Besides, the absorbance changes during the experiment are quite small ($\Delta A = A_{83} - A_{64} = 0.01$). These findings altogether indicate high structural stability of insulin against temperature which could be the result of three disulfide bonds in the protein [41]. Studies have demonstrated that addition of the disulfide bond resulted in a 34.6 °C increase in the melting point of insulin [42]. Moreover, hexameric form of insulin is the most stable form. The standard free energy change

for insulin at 298K ($\Delta G^\circ(298K)$) was obtained +88.2 kJ/mol based on Pace analysis [31].

In order to determine the role of surfactant in the thermal stability of insulin, this experiment was performed in the presence of various concentrations of S_6 (Fig. 7). The presence of S_6 and the complex formation made insulin more stable (in accord with the far-UV CD data), as full sigmoidal denaturation curve was not observed.

Particles size measurements

The size of S_6 micelles and S_6 -insulin complexes with different surfactant concentrations, were measured

Table 3. The mean diameter of S₆-insulin complexes in different S₆ concentration ([S₆]/[Ins]= 0, 3, 5, 7, 9, 10).

Samples	Mean diameter (nm)	PDI*
micelles	156.8 ^a	-
[S ₆]/[Ins]= 0	180.4 ± 1.2 ^b	0.137
[S ₆]/[Ins]= 3	162.4 ± 1.5	0.089
[S ₆]/[Ins]= 5	155.4 ± 1.7	0.091
[S ₆]/[Ins]= 7	133.8 ± 0.2	0.200
[S ₆]/[Ins]= 9	127.0 ± 1.6	0.116
[S ₆]/[Ins]= 10	121.2 ± 0.2	0.181

*Poly Dispersity Index

^a Mean diameter of two independent experiments.^bStandard error

by DLS and the data are listed in Table 3. Hydrodynamic diameter of S₆ micelles is the average value of two independent measurements. Results show, that the size of complexes, decrease with increasing surfactant concentration, probably because of hexamer dissociation in the presence of the surfactant. This result confirms the near-UV CD data.

Zeta potential measurements

In order to get an idea about the variations of the charges in the S₆-insulin complexes as a function of [S₆]/[Ins] ratio, zeta potential measurements were performed at pH 7.40. Fig. 8 is a plot of ζ-potential versus [S₆]/[Ins] ratio. The net charge of insulin at pH, 7.40 is negative (pI, 5.30). The S₆-protein complex with the molar ratio 3, ([S₆]/[Ins]=3), shows a more negative surface charge compared with insulin. According to near-UV CD, this is probably because of the dissociation of hexamer to its smaller oligomers, which leads to exposure of negatively charged surfaces. In [S₆]/[Ins]= 5, the surface charges of the complex becomes positive, as a result of charge neutralization of protein by the cationic surfactant. With increasing surfactant concentration ([S₆]/[Ins]= 7, 9, 10), the positive charge decreases and finally becomes almost zero. This is maybe because of the orientation effects of the protein and the surfactant.

Summary of the results shows that: This cationic gemini surfactant (S₆) creates spherical self-assembling nanostructures (micelle) in biological environments. S₆ forms a complex with insulin and causes both static and dynamic quenching of the protein fluorescence. The surfactant increases the structural stability of insulin and consequently decreases the solvent accessibility of Tyr residues. Furthermore, S₆ causes the dissociation of insulin hexameric form (to its active form) with no significant changes in tertiary structure. Several studies have shown that cationic carriers have relatively high cytotoxicity. Therefore, complex charge neutralization which takes place in aqueous solution (pH, 7.40) in the

presence of S₆ is a valuable feature of this carrier [45, 46]. Finally, S₆ can be a candidate for insulin delivery.

Acknowledgment

The authors thank the Iran National Science Foundation (INSF) and Research Council of University of Tehran for their financial support.

References

1. Célia M.C. Faustino, António R.T. Calado and Garcia-Rio L., Gemini surfactant-protein interactions: effect of pH, temperature and surfactant stereochemistry. *Biomacromolecules* **10**: 2508–2514 (2009).
2. Sadatmousavi P., Kovalenko E. and Chen P., Thermodynamic characterization of the interaction between a peptide-drug complex and serum proteins. *Langmuir* **30**: 11122–11130 (2014).
3. Paul B.K., Ghosh N. and Mukherjee S., Binding interaction of a prospective chemotherapeutic antibacterial drug with β-Lactoglobulin: results and challenges. *Langmuir* **30**: 5921–5929 (2014).
4. Bund T., Boggs J.M., Harauz G., Hellmann N. and Hinderberger D., Copper uptake induces self-assembly of 18.5 kDa myelin basic protein (MBP). *Biophysical J.* **99**: 3020–3028 (2010).
5. Gull N., Sen P., Khan R.H. and Kabir-ud-Din. Interaction of bovine (BSA), rabbit (RSA), and porcine (PSA) serum albumins with cationic single-chain/gemini surfactants: a comparative study. *Langmuir* **25**: 11686–11691 (2009).
6. Deo N., Jockusch S., Turro N.J. and Somasundaran P., Surfactant interactions with zein protein. *Langmuir* **19**: 5083–5088 (2003).
7. Andersen K.K., Westh P. and Otzen D.E., Global study of myoglobin-surfactant interactions. *Langmuir* **24**: 399–407 (2008).
8. Gebicka L. and Banasiak E., Interactions of anionic surfactants with methemoglobin. *Colloid Surface B* **83**: 116–121 (2011).
9. Otzen D., Protein-surfactant interactions: a tale of many states. *Biochim. Biophys. Acta* **1814**: 562–591 (2011).

10. Gelamo E.L. and Tabak M., Spectroscopic studies on the interaction of bovine (BSA) and human (HSA) serum albumins with ionic surfactants. *Spectrochim. Acta A* **56**: 2255 – 2271 (2000).
11. Menger F.M. and Keiper J.S., Gemini surfactants, *Angew. Chem. Int. Ed.* **39**: 1906-1920 (2000).
12. Menger F.M. and Littau C.A., Gemini surfactants: a new class of self-assembling molecules. *J. Am. Chem. Soc.* **115**: 10083-10090 (1993).
13. Rosena M.J. and Tracy D.J., Gemini surfactants. *J. Surfactants Deterg.* **1**: 547-554 (1998).
14. Chen Z., Liu G., Chen M., Peng Y. and Wu M., Determination of nanograms of proteins based on decreased resonance light scattering of zwitterionic gemini surfactant. *Anal. Biochem.* **384**: 337–342 (2009).
15. Gull N., Mir M.A., Khan J.M., Khan R.H., Rather G.M. and Dar A.A., Refolding of bovine serum albumin via artificial chaperone protocol using gemini surfactants. *J. Colloid Interface Sci.* **364**: 157–162 (2011).
16. Mohammed-Saeid W., Michel D., El-Aneed A., Verrall R.E., Low N.H. and Badea I., Development of lyophilized gemini surfactant-based gene delivery systems: influence of lyophilization on the structure, activity and stability of the lipoplexes. *J. Pharm. Pharm. Sci.* **15**: 548-567 (2012).
17. Kirby A.J., Camilleri P., Engberts J.B., Feiters M.C., Nolte R.J., Söderman O., Bergsma M., Bell P.C., Fielden M.L., Garcia Rodríguez C.L., Guédat P., Kremer A., McGregor C., Perrin C., Ronsin G. and van Eijk M.C., Gemini surfactants: new synthetic vectors for gene transfection. *Angew. Chem. Int. Ed.* **42**: 1448 – 1457 (2003).
18. Bombelli C., Giansanti L., Luciani P. and Mancini G., Gemini surfactant based carriers in gene and drug delivery. *Curr. Med. Chem.* **16**: 171-183 (2009).
19. Guo Y., Liu J., Zhang X., Feng R., Li H., Zhang J., Lv X. and Luo P., Solution property investigation of combination flooding systems consisting of gemini–non-ionic mixed surfactant and hydrophobically associating polyacrylamide for enhanced oil recovery. *Energ. Fuel.* **26**: 2116–2123 (2012).
20. Wanga F., Chen X., Xu Y., Hu S. and Gao Z., Enhanced electron transfer for hemoglobin entrapped in a cationic gemini surfactant films on electrode and the fabrication of nitric oxide biosensor. *Biosens. Bioelectron.* **23**: 176–182 (2007).
21. Bombelli C., Caracciolo G., Profio P.D., Diociaiuti M., Luciani P., Mancini G., Mazzuca C., Marra M., Molinari A., Monti D., Toccaceli L. and Venanzi M., Inclusion of a photosensitizer in liposomes formed by DMPC/gemini surfactant: correlation between physicochemical and biological features of the complexes. *J. Med. Chem.* **48**: 4882–4891 (2005).
22. Wang Y., Guo R. and Xi J., Comparative studies of interactions of hemoglobin with single-chain and with gemini surfactants. *J. Colloid Interf. Sci.* **331**: 470–475 (2009).
23. Tardioli S., Bonincontro A., Mesa C.L. and Muzzalupo R., Interaction of bovine serum albumin with gemini surfactants. *J. Colloid Interf. Sci.* **347**: 96–101 (2010).
24. Amiri R., Bordbar A.K., Garcia-Mayoral M.F., Khosropour A.R., Mohammadpoor-Baltork I., Menéndez M. and Laurents D.V., Interactions of gemini surfactants with two model proteins: NMR, CD, and fluorescence spectroscopies. *J. Colloid Interf. Sci.* **369**: 245–255 (2012).
25. Litwack G., Insulin and IGFs, Vitamins & Hormones Volume 80, first Ed. Academic press in an imprint of Elsevier, New York, (2009).
26. Walsh G. and Murphy B., Biopharmaceuticals, an Industrial Perspective, Kluwer academic publishers, Netherlands, (1999).
27. Whittingham J.L., Scott D.J., Chance K., Wilson A., Finch J., Brange J. and Dodson G.G., Insulin at pH 2: structural analysis of the conditions promoting insulin fibre formation. *J. Mol. Biol.* **318**: 479-490 (2002).
28. Uversky V.N., Nielsen Garriques L., Millett I.S., Frokjaer S., Brange J., Doniach S. and Fink A.L., Prediction of the association state of insulin using spectral parameters. *J. Pharm. Sci.* **92**: 847-858 (2003).
29. Pourhosseini P.S., Saboury A.A., Najafi F. and Sarbolouki M.N., Interaction of insulin with a triblock copolymer of PEG-(fumaric-sebacic acids)-PEG: Thermodynamic and spectroscopic studies. *Biochim. Biophys. Acta* **1774**: 1274-1280 (2007).
30. Sambrook J., Fritsch E.F. and Maniatis T., Molecular Cloning, A Laboratory Manual, 2nd Ed., CSH (Cold Spring Harbor Laboratory Press), New York, (1989).
31. Pace C. N., Measuring and increasing protein stability. *Tibtech* **8**: 93-98 (1990).
32. Ahmad A., Millett I.S., Doniach S., Uversky V.N. and Fink A.L., Partially folded intermediates in insulin fibrillation. *Biochemistry* **42**: 11404-11416 (2003).
33. Burstein E.A., Intrinsic protein fluorescence: origin and applications, VINITI, Moscow, (1976).
34. Pecora R., Dynamic light scattering: applications of photon correlation spectroscopy, Plenum Press, New York, (1985).
35. Hunter R.J., Zeta potential in colloid science: principles and applications, Ottewill R.H., Rowel R.L. (Eds.), Academic Press, New York, (1981),
36. Liu W., Guo X. and Guo R., The interaction between hemoglobin and two surfactants with different charges. *Int. J. Biol. Macromol.* **41**: 548-557 (2007).
37. Williams R.J., Phillips J.N. and Mysels K.J., The critical micelle concentration of sodiumlaurylsulphate at 25 . *Trans. Faraday Soc.* **51**: 728-737 (1955).
38. Saboury A.A. and Moosavi-Movahedi A.A., Derivation of the thermodynamic parameters involved in the elucidation of protein thermal profiles. *Biochem. Educa.* **23**: 164-168 (1995).
39. Lakowicz J.R., Principles of fluorescence spectroscopy, third Ed., springer science/ Business media, New York, (2006).
40. Ahmad A., Uversky V.N., Hong D. and Fink A.L., Early events in the fibrillation of monomeric insulin. *J. boil. Chem.* **280**: 42669-42675 (2005).
41. Huus K., Havelund S., Olsen H.B., Weert M. and Frokjaer S., Thermal dissociation and unfolding of insulin. *Biochemistry* **44**: 11171-11177 (2005).
42. Vinther T.N., Norrman M., Ribell U., Huus K., Schlein M., Steensgaard D.B., Pedersen T.A., Pettersson I., Ludvigsen S., Kjeldsen T., Jensen K.J. and Hubalek F.,

- Insulin analog with additional disulfide bond has increased stability and preserved activity. *Protein sci.* **22**: 296-305 (2013).
43. Ahmad A., Millett I.S., Doniach S., Uversky V.N. and Fink A.L., Stimulation of Insulin Fibrillation by Urea-induced Intermediates. *J. boil. Chem.* **279**: 14999-15013 (2004).
44. Uversky V.N., Garriques L.N., Millett I.S., Frokjaer S., Brange J., Doniach S. and Fink A.L., Prediction of the association state of insulin using spectral parameters. *J. Pharm. Sci.* **92**: 847-858 (2003).
45. Moghimi S.M, Symonds P., Murray J.C., Hunter A.C., Debska G. and Szewczyk A., A two-stage poly(ethylenimine)-mediated cytotoxicity: implications for gene transfer/therapy. *Molecular Therapy* **11**: 990-995 (2005).
46. Hunter A.C. and Moghimi S.M., Cationic carriers of genetic material and cell death: a mitochondrial tale. *(BBA)-Bioenergetics* **1797**: 1203-1209 (2010).